Supporting Information for

Green Solvent-Processed, High-Performance Organic Solar Cells Achieved by Outer Side-Chain Selection of Selenophene-Incorporated Y-Series Acceptors

Changkyun Kim,[a,†] *Shuhao Chen,*[b,†] *Jin Su Park,*[a] *Geon-U Kim,*[a] *Hyunbum Kang,*[a] *Seungjin Lee,*[a] *Tan Ngoc-Lan Phan,*[a] *Soon-Ki Kwon,*[c,*] *Yun-Hi Kim,*[b,*] *and Bumjoon J. Kim*[a,*]

[a] Department of Chemical and Biomolecular Engineering, Korea Advanced Institute of Science and Technology (KAIST), Daejeon 34141, Republic of Korea.

[b] Department of Chemistry and RIGET, Gyeongsang National University, Jinju 52828, Republic of Korea

[c] Department of Materials Engineering and Convergence Technology and ERI, Gyeongsang National University and ERI, Jinju 52828, Republic of Korea.

[*](B. J. Kim) E-mail: bumjoonkim@kaist.ac.kr

[*](Y.-H. Kim) E-mail: ykim@gnu.ac.kr

[*](S.-K. Kwon) E-mail: skwon@gnu.ac.kr

Table of Contents

Supplementary Table S1-7

- **Table S1:** Elemental analysis of YSe-Cx SMAs.
- **Table S2:** Photovoltaic properties of optimized PM6:YSe-C9 devices with different inner side-chains.
- **Table S3:** Photovoltaic properties of optimized PM6:YSe-Cx devices with different non-halogenated solvents.
- **Table S4:** Contact angle and surface energy of PM6 and YSe-Cx pristine films processed with o-xylene. Flory–Huggins interaction parameters (χ) between PM6 and YSe-Cx in each blend.
- **Table S5:** Melting temperatures and enthalpies in 1st heating thermogram of YSe-Cx-based pristine and blend films processed with *o*-xylene.
- **Table S6:** Photovoltaic properties of optimized PM6:YSe-Cx devices with different thicknesses of active layers.
- **Table S7:** SCLC hole and electron mobilities of PM6:YSe-Cx devices with different thicknesses of active layers.

Experimental Section

Materials

For the synthesis of YSe-Cx (x = 3, 6, or 9), the starting chemical reagents were purchased from Alfa Aesar, TCI and Aldrich. The starting materials and solvents were further purified prior to use. Poly(3,4-ethylenedioxythiophene):poly(styrenesulfonate) (PEDOT:PSS) (Clevios P VP AI 4083) solution was bought from Heraeus (Germany) to fabricate a hole-transporting layer. As a polymer donor, PM6 was purchased from Brilliant Matters. For an electron-transporting layer, 2,9-bis(3-((3-(dimethylamino)propyl)amino)propyl)anthra[2,1,9-*def*:6,5,10-*d'e'f'*]diisoquinoline-1,3,8,10(2*H*,9*H*)-tetraone (PDINN) was synthesized by following the method in the previous report.[1]

Characterizations

^{1}H-NMR and ^{13}C-NMR analysis were conducted with a Bruker DRX-300 and DRX-500 MHz spectrometer, and chemical shifts were recorded in a ppm unit. The matrix-assisted laser desorption/ionization-time of flight (MALDI-TOF) mass spectra analysis was conducted using 4800 MALDI-TOF/TOF mass analyzer and SCIEX Voyager DE-STR. Cyclic voltammograms were measured with a PowerLab/AD instrument. Ag/AgCl electrode, Pt wire, and glassy carbon electrode were used as the reference electrode, counter electrode, and the working electrode, respectively. The solution with 0.1 M tetrabutylammonium hexafluorophosphate in acetonitrile was used as the electrolyte, at a scan rate of 50 mV s^{-1}. Grazing incidence wide angle X-ray scattering (GIWAXS) was measured at 9A Beamline in Pohang Accelerator Laboratory (South Korea), with incidence angles between 0.08 – 0.13°. Based on the optimized device fabrication conditions, the active layer layers were solution-processed onto the Si/PEDOT:PSS substrates for the GIWAXS measurement. For quantitative analysis for each scattering peak, the L_c values were calculated using the Scherrer equation:[2, 3]

$$L_c = \frac{2\pi K}{\Delta q} \quad (1)$$

where K indicates the shape factor (was set to 0.9 in this paper) and Δq means the full-width at half-maximum of each scattering peak, respectively. Atomic force microscropy height images (AFM, MultiMode 8, Bruker) were obtained under ambient conditions to investigate the blend morphologies and film thicknesses. The contact angles of water and glycerol onto pristine films of PM6 and YSe-Cx were measured using a contact angle analyzer (DSA, KRUSS). The surface tension of the film relative to two solvents (water, and glycerol) was calculated using the Wu model in the following method[4]:

$$\gamma_{water}\ (1 + \cos\theta_{water}) = 4 \times \frac{\gamma_{water}^{d}\gamma^{d}}{\gamma_{water}^{d}+\gamma^{d}} + 4 \times \frac{\gamma_{water}^{p}\gamma^{p}}{\gamma_{water}^{p}+\gamma^{p}} \quad (2)$$

$$\gamma_{glycerol}\ (1 + \cos\theta_{glycerol}) = 4 \times \frac{\gamma_{glycerol}^{d}\gamma^{d}}{\gamma_{gylcerol}^{d}+\gamma^{d}} + 4 \times \frac{\gamma_{glycerol}^{p}\gamma^{p}}{\gamma_{gylcerol}^{p}+\gamma^{p}} \quad (3)$$

$$\gamma^{total} = \gamma^{d} + \gamma^{p} \quad (4)$$

where γ^{total} is the total surface tension of the materials that is obtained from the sum of dispersion part γ^{d} and polar part γ^{p}. The solubility parameter (δ) of the material was estimated based on the previous literature.[5] Flory-Huggins interaction parameter (χ) between donor and acceptor materials was calculated from the δ values using the following relation[6]:

$$\gamma_{donor-acceptor} = \frac{V_1}{RT}(\delta_{donor} - \delta_{acceptor})^2 + 0.34 \quad (5)$$

where V_1 is the solvent molar volume. The term 0.34 originates from the entropic contribution.[7] Differential scanning calorimetry (DSC, TA Instrument) thermograms were obtained to investigate the thermal properties of the pristine and blend films of PM6 and different SMAs.

OSC Fabrication

The conventional type OSC was fabricated with the structure of indium tin oxide (ITO)/ PEDOT:PSS/PM6:YSe-Cx/PDINN/Ag.[1] Before fabrication, the ITO substrates were rinsed with sonication using acetone, deionized water, and isopropyl alcohol sequentially. Then, the substrates were desiccated in the oven at 80 ^{o}C for 25 min. After the ITO substrates were plasma-treated for 10 min, the PEDOT:PSS solution (AI4083) was spin-coated at 3000 rpm for 40 s. Then, the substrates were thermally annealed at 165 ^{o}C for 30 min in the ambient condition. The blend solution for the active layers of about 95 nm thickness was prepared with 10 mg mL^{-1} of PM6 concentration and 1:1 (w/w) ratio of PM6:YSe-Cx in *o*-xylene. After stirring the solution at 110 ^{o}C for 1 hr, it was spin-coated on the ITO/PEDOT:PSS substrate at 2000 rpm for 40 s. To remove the remaining solvent, the active layers were dried under high vacuum condition (10^{-6} Torr) overnight. The PDINN was then dissolved in methanol (1.0 mg mL^{-1}) and spin-coated on the active layer in 3000 rpm, followed by 120 nm-thick Ag electrode deposition. For the active layer thickness tolerance experiments, the concentration of the blend solution was adjusted to 40 mg mL^{-1} and the solution was spin-coated at 500 rpm to produce 400 nm thick film with high uniformity. The 200 nm and 300 nm-thick active layer films were also produced by spin-coating the solution with a 40 mg mL^{-1} concentration, but different spinning rates. The 200 nm-thick film was formed by spin-coating at 900 rpm while the 300 nm-thick film was prepared at 2000 rpm. Using an optical microscope, the area of active layers for OSC devices was measured to be 0.042 cm^2.

OSC Characterization

Under AM 1.5G solar irradiance (100 mW cm^{-2}), the *J–V* curves were measured in ambient conditions (K201 LAB55, McScience). The solar simulator satisfies ASTM standard AAA rating. The solar simulator was calibrated using a silicon reference cell (K801S-K302, McScience). External quantum efficiency (EQE) spectra were measured by an instrument (K3100 IQX, McScience, Inc.) equipped with a 300 W Xenon arc lamp filtered by an optical chopper (MC2000, Thorlabs) and a monochromator (Newport). The calculated J_{sc} values were acquired from the EQE measurements by integrating the AM 1.5G solar spectra from 300 to 1000 nm wavelength. All the calculated J_{sc} values from the EQE spectra were matched well with the measured J_{sc} values within a 3% error.

By using the SCLC method, the charge mobilities of the PM6:YSe-Cx blend active layers with several thicknesses were measured with a hole-only device architecture of ITO/PEDOT:PSS/PM6:YSe-Cx/Au (80 nm) and an electron-only device architecture of ITO/zinc oxide (ZnO)/blend film/Ca (20 nm)/Al (80 nm). Current–voltage measurements were measured in the range of 0–6 V, and the results were connected with the Mott–Gurney equation as follows:

$$J_{SCLC} = \frac{9}{8}\varepsilon\varepsilon_0\mu\frac{V^2}{L^3},$$

where ε_0 is the vacuum space permittivity, ε is the blend film dielectric constant, μ is the charge mobility, V is the potential across the device related to the loss of potential due to the series resistance V_{rs} of the electrode and built-in potential V_{bi} ($V = V_{appl} - V_{rs} - V_{bi}$), and L is the thickness of blend film.[8]

Synthesis

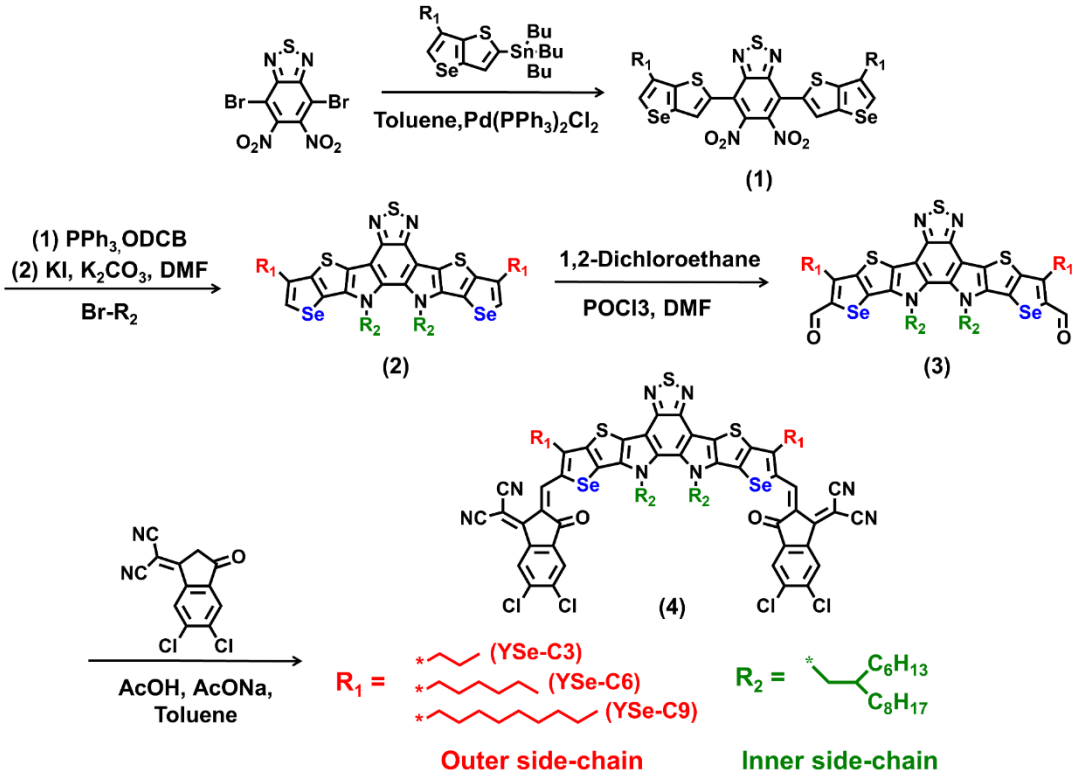

Scheme S1. Synthetic scheme for YSe-Cx SMAs.

Synthesis of 5,6-dinitro-4,7-bis(6-alkylselenopheno[3,2-b]thiophen-2-yl)benzo[c][1,2,5] thiadiazole (1a-c)

For the synthesis of **1a**, to a mixture of tributyl(6-propylselenopheno[3,2-*b*]thiophen-2-yl) stannane (15.0 g, 28.8 mmol) and compound 4,7-dibromo-5,6-dinitrobenzo[*c*][1,2,5] thiadiazole (5.1 g, 13.1 mmol) in anhydrous toluene (100 mL), bis(triphenylphosphin e)palladium(II) dichloride ($Pd(PPh_3)Cl_2$) (0.41 g, 0.58 mmol) was added under nitrogen atmosphere. The mixture was stirred and refluxed overnight. The crude product was washed with deionized (DI) water and dried with $MgSO_4$. After the filtration of $MgSO_4$, remaining toluene was evaporated in vacuum. The crude was further purified with silica gel column chromatography using blend eluent based on *n*-hexane/methylene chloride (DCM) (v/v = 3:1) to get the compound **1a** as a red solid (yield: 4.3 g, 48%). **1b** and **1c** were also synthesized following this procedure**.**

1a: ^{1}H NMR ($CDCl_3$, 300MHz, ppm): δ 7.78 – 7.60 (m, 4H), 2.67 (td, *J* = 7.8, 0.9 Hz, 4H), 1.75 (dq, *J* = 14.7, 7.3 Hz, 4H), 0.95 (t, *J* = 7.3 Hz, 6H). ^{13}C NMR ($CDCl_3$, 500MHz, ppm): δ 152.2, 146.5, 137.8, 136.9, 129.6, 128.2, 127.2, 121.3, 33.4, 21.8, 13.7. HRMS (m/z): [M] calcd for $C_{24}H_{18}N_4O_4S_3Se_2$, 681.8821, found, 681.8819.

1b: ^{1}H NMR ($CDCl_3$, 300MHz, ppm): δ 7.81 – 7.70 (m, 4H), 2.76 (t, *J* = 8.0 Hz, 4H), 1.86 – 1.73 (m, 4H), 1.38-1.27 (m, 12H), 0.99 – 0.87 (m, 6H). ^{13}C NMR ($CDCl_3$, 500MHz, ppm): δ 152.2, 146.7, 141.7, 137.8, 127.9, 127.1, 121.1, 31.9, 31.4, 29.6, 29.4, 29.3, 28.4, 22.6, 14.2. HRMS (m/z): [M] calcd for $C_{30}H_{30}N_4O_4S_3Se_2$, 765.9760, found, 765.9758.

1c: ^{1}H NMR ($CDCl_3$, 300MHz, ppm): δ 7.79 – 7.57 (m, 4H), 2.68 (t, *J* = 7.6 Hz, 4H), 1.71 (dt, *J* = 14.8, 7.4 Hz, 4H), 1.20 (s, 24H), 0.78 (d, *J* = 6.9 Hz, 6H). ^{13}C NMR ($CDCl_3$, 500MHz, ppm): δ 152.2, 146.7, 141.7, 137.8, 137.1, 129.5, 127.9, 127.1, 121.1, 31.9, 31.4, 29.6, 29.4, 29.3, 28.4, 22.6, 14.2. HRMS (m/z): [M] calcd for $C_{36}H_{42}N_4O_4S_3Se_2$, 850.0699, found, 851.0766.

Synthesis of 12,13-bis(2-hexyldecyl)-3,9-dialkyl-12,13-dihydroselenopheno[2'',3'':4',5'] thieno[2',3':4,5]pyrrolo[3,2-g]selenopheno[2',3':4,5]thieno[3,2-b][1,2,5]thiadiazolo[3,4-e] indole (2a-c)

For the synthesis of **2a**, to the solution of compound **1a** (4.1 g, 5.87 mmol) with *o*-dichlorobenzene (*o*-DCB) solvent (50 mL), triphenylphosphine (PPh_3) (8.0 g, 30.5 mmol) was added under nitrogen atmosphere. Then the mixture was stirred and refluxed for 24 hours. After removal of the solvent by distillation, the mixture was washed by water. After crude product was dried over anhydrous $MgSO_4$, the solvent was removed by rotary evaporator to obtain deep red solid. Without further purification, to the mixture of crude compound (1.27 g), K_2CO_3 (1 g, 7.12 mmol) and KI (0.43 g, 2.63 mmol) in anhydrous dimethylformamide (DMF) (30 mL), 7-(bromomethyl) pentadecane (2.46 g, 8.09 mmol) was added dropwisely under nitrogen atmosphere. The mixture was stirred and refluxed overnight. The reaction was quenched and washed by DI water. The organic phase was dried over anhydrous $MgSO_4$ and the solvent was removed in vacuum. The crude was purified on a silica gel column chromatography using n-hexane/DCM (v/v = 3:1) as the blend eluent to obtain the compound **2a** as an orange solid (final yield: 1.26 g, 20%). **2b** and **2c** were also synthesized following this procedure**.**

2a: ^{1}H NMR ($CDCl_3$, 300MHz, ppm): δ 7.72 – 7.54 (m, 2H), 4.62 (d, *J* = 7.7 Hz, 4H), 2.83 (t, *J* = 7.4 Hz, 4H), 2.19 – 2.07 (m, 2H), 1.99 – 1.86 (m, 4H), 1.26 – 0.66 (m, 66H). ^{13}C NMR ($CDCl_3$, 500MHz, ppm): δ 161.2, 147.7, 253.3, 140.3, 138.4, 132.1, 122.3, 122.2, 122.0, 111.2, 66.5, 38.7, 37.3, 31.8, 31.6, 29.3, 29.1, 22.6, 22.5, 22.0, 13.9, 13.8, 13.7. HRMS (m/z): [M] calcd for $C_{56}H_{82}N_4S_3Se_2$, 1066.4032, found, 1066.4026.

2b: ^{1}H NMR ($CDCl_3$, 300MHz, ppm): δ 7.51 (s, 2H), 4.50 (d, *J* = 7.8 Hz, 4H), 2.76 – 2.68 (m, 4H), 2.00 (dd, *J* = 12.6, 7.7 Hz, 2H), 1.78 (dt, *J* = 15.3, 7.8 Hz, 4H), 1.35 – 0.54 (m, 78H). ^{13}C NMR ($CDCl_3$, 500MHz, ppm): δ 161.3, 147.6, 143.3, 140.3, 138.6, 132.2, 122.3, 111.0,

66.5, 38.7, 37.0, 31.8, 31.6, 31.0, 29.7, 29.2, 29.1, 28.8, 22.6, 22.5, 13.9, 13.7. HRMS (m/z): [M] calcd for $C_{62}H_{94}N_4S_3Se_2$, 1150.4971, found, 1151.5053.

2c: ^{1}H NMR ($CDCl_3$, 300MHz, ppm): δ 7.49 (s, 2H), 4.49 (d, *J* = 7.7 Hz, 4H), 2.71 (t, *J* = 7.7 Hz, 4H), 2.04 – 1.95 (m, 2H), 1.83 – 1.69 (m, 4H), 1.42 – 0.52 (m, 90H). ^{13}C NMR ($CDCl_3$, 500MHz, ppm): δ 147.6, 143.4, 140.4, 138.6, 132.1, 122.2, 122.0, 111.2, 38.7, 31.9, 31.8, 31.6, 29.7, 29.4, 29.3, 28.8, 22.7, 22.6, 22.5, 13.9, 13.7. HRMS (m/z): [M] calcd for $C_{68}H_{106}N_4S_3Se_2$, 1234.5910, found, 1235.5982.

Synthesis of 12,13-bis(2-hexyldecyl)-3,9-dialkyl-12,13-dihydroselenopheno[2'',3'':4',5'] thieno[2',3':4,5]pyrrolo[3,2-g]selenopheno[2',3':4,5]thieno[3,2-b][1,2,5]thiadiazolo[3,4-e] indole-2,10-dicarbaldehyde (3a-c)

For the synthesis of **3a**, to a solution of compound **2a** (1.10 g, 1.03 mmol) and anhydrous DMF (1.51 g, 20.6 mmol) in dichloroethane (DCE) (30 mL), phosphoryl chloride ($POCl_3$) (3.17 g, 20.6 mmol) was added dropwisely under nitrogen atmosphere while maintaining the flask temperature with -78 °C. Then the mixture was stirred and refluxed overnight. The reaction was quenched with sodium acetate solution (1 M in water, 100 mL) and crude product was extracted by ethyl acetate. The organic phase was dried over anhydrous $MgSO_4$ and the solvent was removed by evaporator. The crude was purified on a silica gel column chromatography using *n*-hexane/DCM (v/v = 1:1) as the eluent to obtain the compound **3a** as an orange solid (yield: 0.98 g, 85%).

3a: ^{1}H NMR ($CDCl_3$, 300MHz, ppm): δ 9.96 (s, 2H), 4.54 (d, *J* = 7.8 Hz, 4H), 3.18 – 3.04 (m, 4H), 2.01 – 1.82 (m, 6H), 1.29 – 0.52 (m, 66H). ^{13}C NMR ($CDCl_3$, 500MHz, ppm): δ 182.4, 148.8, 147.6, 144.5, 141.4, 140.5, 133.5, 129.3, 128.3, 126.6, 112.0, 38.9, 31.8, 31.6, 29.4, 29.3, 23.9, 22.6, 22.5, 13.9, 13.7. HRMS (m/z): [M] calcd for $C_{58}H_{82}N_4O_2S_3Se_2$, 1122.3930, found, 1122.3946.

3b: ^{1}H NMR ($CDCl_3$, 300MHz, ppm): δ 10.04 (s, 2H), 4.59 (d, *J* = 7.7 Hz, 4H), 3.19 (t, *J* = 7.8 Hz, 4H), 2.10 – 2.00 (m, 2H), 1.93 (dd, *J* = 15.3, 7.8 Hz, 4H), 1.54 – 0.61 (m, 78H). ^{13}C NMR ($CDCl_3$, 500MHz, ppm): δ 182.5, 149.2, 147.6, 141.1, 140.5, 133.3, 128.5, 126.8, 112.1, 55.0, 39.0, 31.8, 31.6, 31.5, 29.4, 29.1, 22.6, 22.5, 14.1, 14.0. HRMS (m/z): [M] calcd for $C_{64}H_{94}N_4O_2S_3Se_2$, 1206.4869, found, 1206.4869.

3c: ^{1}H NMR ($CDCl_3$, 300MHz, ppm): δ 9.97 (s, 2H), 4.52 (d, J = 7.5 Hz, 4H), 3.11 (t, J = 7.6 Hz, 4H), 1.89 (ddd, J = 22.1, 16.0, 5.9 Hz, 6H), 1.46 – 0.53 (m, 90H). ^{13}C NMR ($CDCl_3$, 500MHz, ppm): δ 182.3, 149.4, 147.4, 144.4, 140.9, 140.2, 133.6, 128.4, 126.6, 111.9, 55.0, 38.9, 31.9, 31.8, 29.4, 29.3, 22.7, 22.6, 22.5, 14.1, 14.0. HRMS (m/z): [M] calcd for $C_{70}H_{106}N_4O_2S_3Se_2$, 1290.5808, found, 1290.5802.

Synthesis of YSe-Cx (x = 3, 6, or 9) (4a-c)

To a mixture of 2-(5,6-dichloro-3-oxo-2,3-dihydro-1*H*-inden-1-ylidene)malononitrile (0.47 g, 1.78mmol) and sodium acetate (0.18 g, 2.14 mmol) in acetic acid (30 mL), a solution of compound **3a** (0.40 g, 0.36 mmol) in anhydrous toluene (20 mL) was added under nitrogen atmosphere. The mixture was stirred and refluxed for 24 hr. Then the reaction was quenched with water and extracted by DCM. The organic phase was dried over anhydrous $MgSO_4$ and the solvent was removed by rotary evaporator. The crude was purified on a silica column chromatography using *n*-hexane/DCM (v/v = 1:1) as the eluent to obtain the compound **4a** as a blue solid (yield: 0.35 g, 61%).

4a: ^{1}H NMR ($CDCl_3$, 300MHz, ppm): δ 9.22 (s, 2H), 8.72 (s, 2H), 7.88 (s, 2H), 4.63 (d, J = 7.7 Hz, 4H), 3.23 – 3.13 (m, 4H), 2.12 – 2.01 (m, 2H), 1.85 – 1.72 (m, 4H), 0.90 (m, 66H). ^{13}C NMR ($CDCl_3$, 500MHz, ppm): δ 206.9, 186.7, 158.6, 156.7, 147.7, 147.6, 141.9, 139.6, 139.0, 138.6, 138.2, 135.9, 134.5, 127.0, 119.3, 115.2, 114.6, 113.5. MALDI-TOF calcd for $C_{82}H_{86}Cl_4N_8O_2S_3Se_2$, 1610.3120, found, 1610.2313.

4b: ^{1}H NMR ($CDCl_3$, 300MHz, ppm): δ 9.30 (s, 2H), 8.79 (s, 2H), 7.96 (s, 2H), 4.71 (d, *J* = 7.7 Hz, 4H), 3.30 – 3.21 (m, 4H), 2.20 – 2.10 (m, 2H), 1.95 – 1.80 (m, 4H), 1.43 – 0.64 (m, 78H). ^{13}C NMR ($CDCl_3$, 500MHz, ppm): δ 186.8, 158.6, 157.2, 142.0, 139.6, 139.1, 138.7, 138.2, 136.0, 134.6, 134.4, 130.4, 127.0, 124.0, 119.1, 115.0, 114.6. 113.6, 68.7, 55.8, 39.0, 31.8, 31.8, 31.6, 29.2, 22.6, 22.5, 14.1, 14.0. MALDI-TOF calcd for $C_{88}H_{98}Cl_4N_8O_2S_3Se_2$, 1694.4059, found, 1694.4937.

4c: ^{1}H NMR ($CDCl_3$, 300MHz, ppm): δ 9.18 (s, 2H), 8.67 (s, 2H), 7.88 (s, 2H), 4.66 (d, 4H), 3.20 – 3.13 (m, 4H), 2.11 – 2.07 (m, 2H), 1.82 – 1.73 (m, 4H), 1.24 – 0.59 (m, 90H). ^{13}C NMR ($CDCl_3$, 500MHz, ppm): δ 186.9, 169.5, 158.5, 157.2, 147.7, 141.9, 139.5, 139.1, 138.8, 138.4, 135.9, 134.6, 130.4, 126.8, 125.0, 119.2, 115.0, 114.6, 113.6, 68.7, 39.0, 31.9, 31.8, 30.9, 29.3, 22.7, 22.6, 22.4, 14.1, 14.0. MALDI-TOF calcd for $C_{94}H_{110}Cl_4N_8O_2S_3Se_2$, 1778.4998, found, 1778.5979

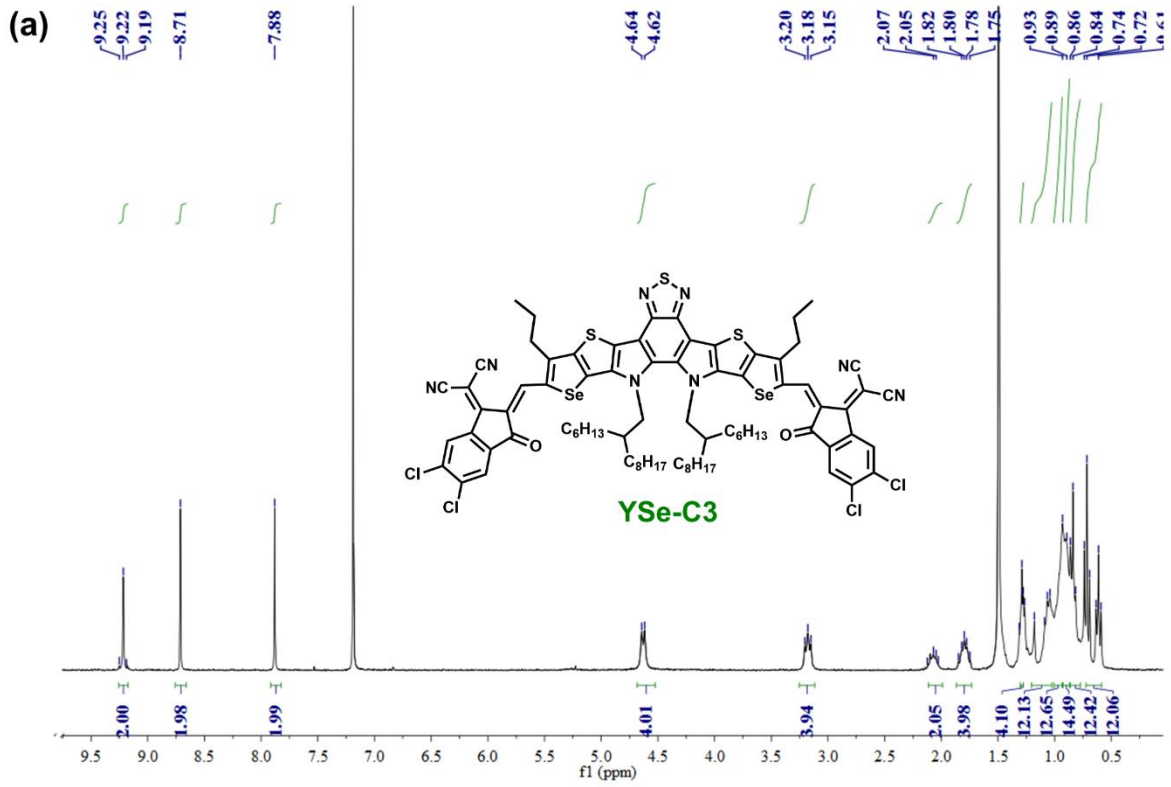
(a)
9.25
9.22
9.19
8.71
7.88
4.64
4.62
3.20
3.18
3.15
2.07
2.05
1.82
1.80
1.78
1.75
0.93
0.89
0.86
0.84
0.74
0.72
YSe-C3
2.00
1.98
1.99
4.01
3.94
2.05
3.98
4.10
12.13
12.65
14.49
12.42
12.06
f1 (ppm)

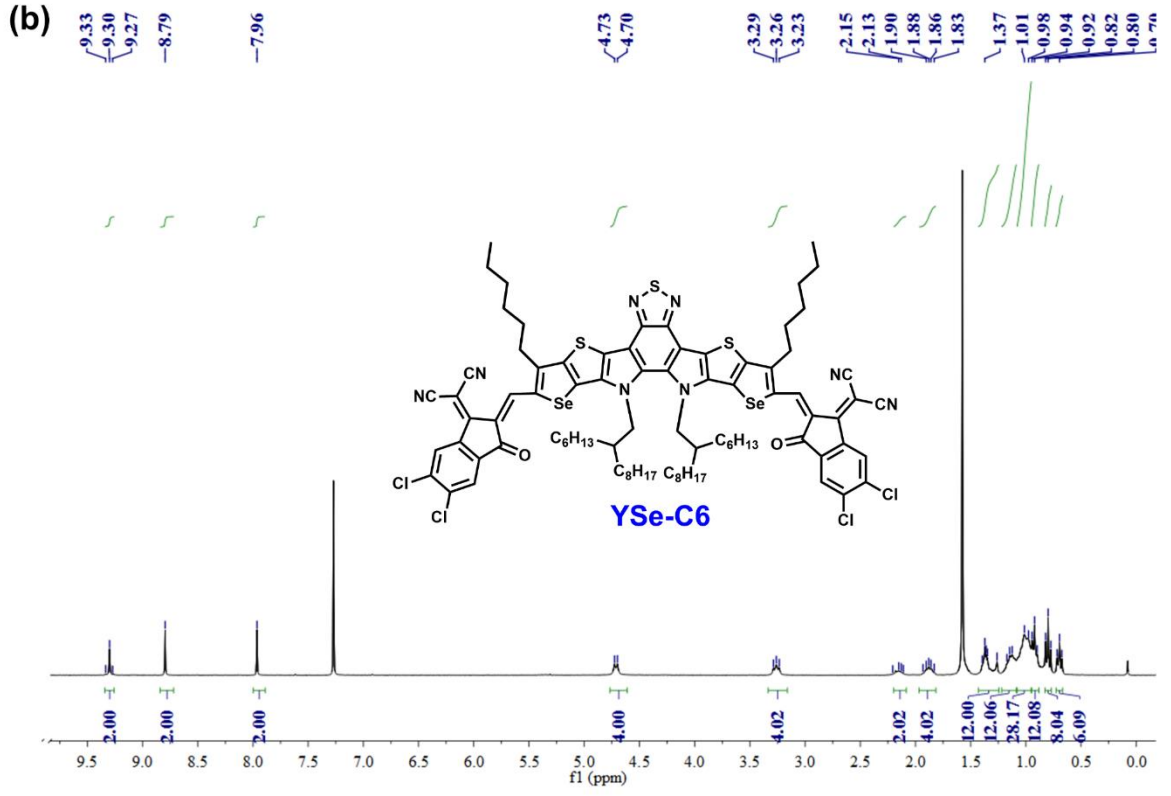
(b)
9.33
9.30
9.27
8.79
7.96
4.73
4.70
3.29
3.26
3.23
2.15
2.13
1.90
1.88
1.86
1.83
1.37
1.01
0.98
0.94
0.92
0.82
0.80
YSe-C6
2.00
2.00
2.00
4.00
4.02
2.02
4.02
12.00
12.06
28.17
12.08
8.04
6.09
f1 (ppm)

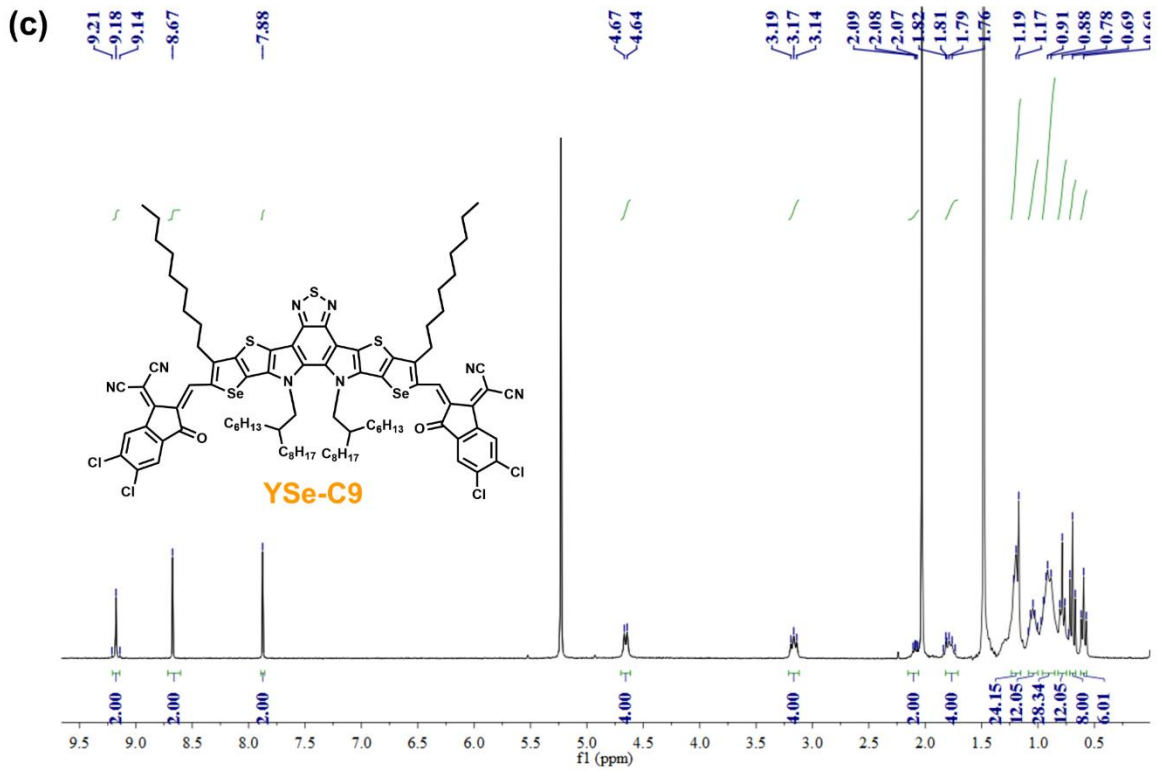

Fig. S1. ^{1}H NMR spectra of (a) YSe-C3, (b) YSe-C6, and (c) YSe-C9 SMAs.

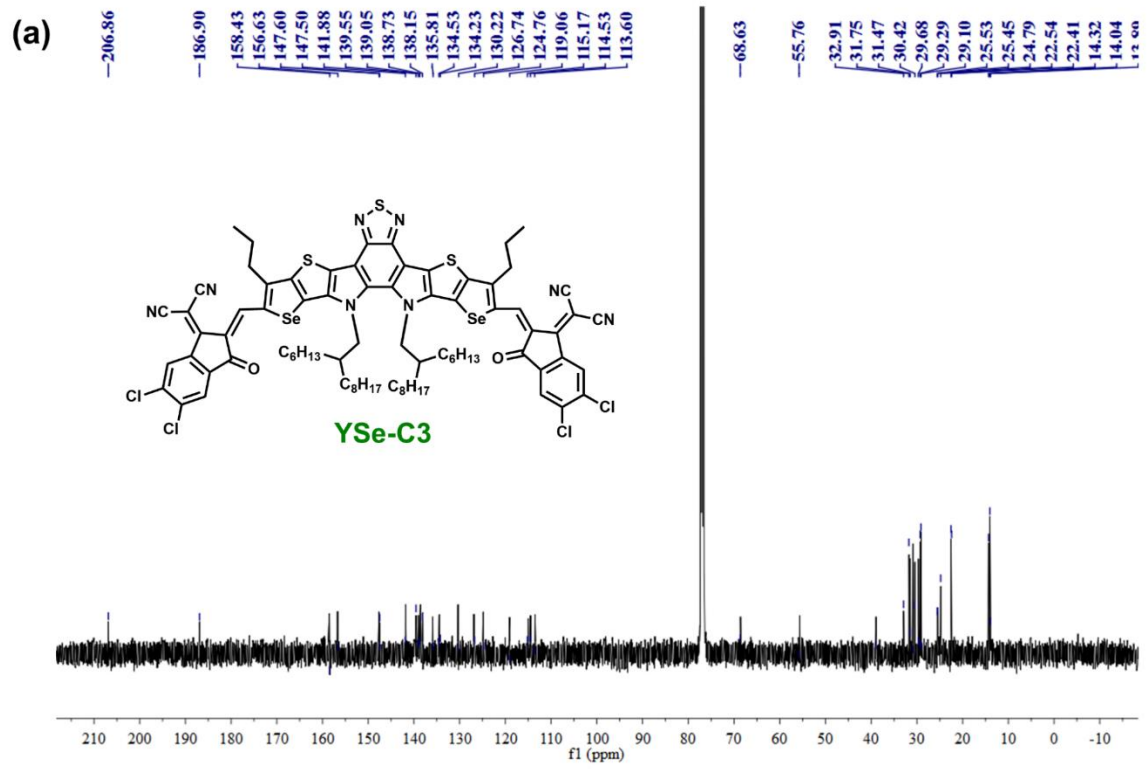
(a)
206.86
186.90
158.43
156.63
147.60
147.50
141.88
139.55
139.05
138.73
138.15
135.81
134.53
134.23
130.22
126.74
124.76
119.06
115.17
114.53
113.60
68.63
55.76
32.91
31.75
31.47
30.42
29.68
29.29
29.10
25.53
25.45
24.79
22.54
22.41
14.32
14.04
YSe-C3
f1 (ppm)

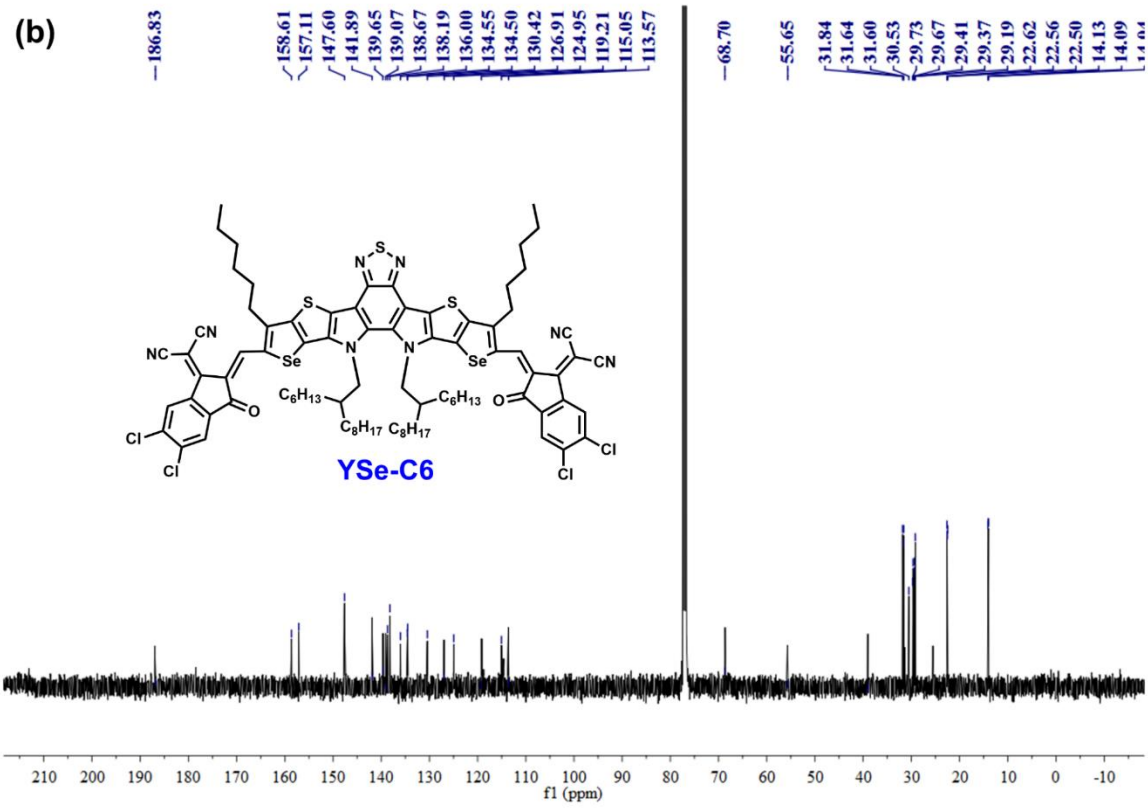
(b)
186.83
158.61
157.11
147.60
141.89
139.65
139.07
138.67
138.19
136.00
134.55
134.50
130.42
126.91
124.95
119.21
115.05
113.57
68.70
55.65
31.84
31.64
31.60
30.53
29.73
29.67
29.41
29.37
29.19
22.62
22.56
22.50
14.13
14.09
YSe-C6
f1 (ppm)

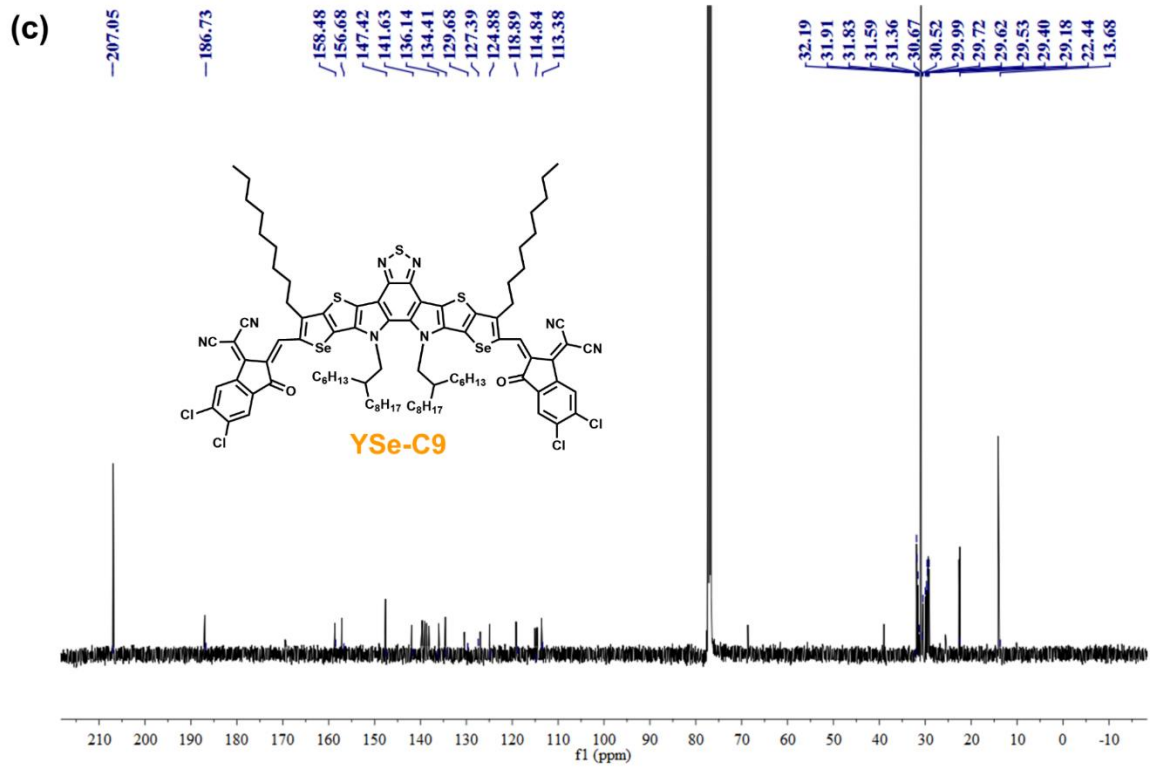

Fig. S2. ^{13}C NMR spectra of (a) YSe-C3, (b) YSe-C6, and (c) YSe-C9 SMAs.

(a)

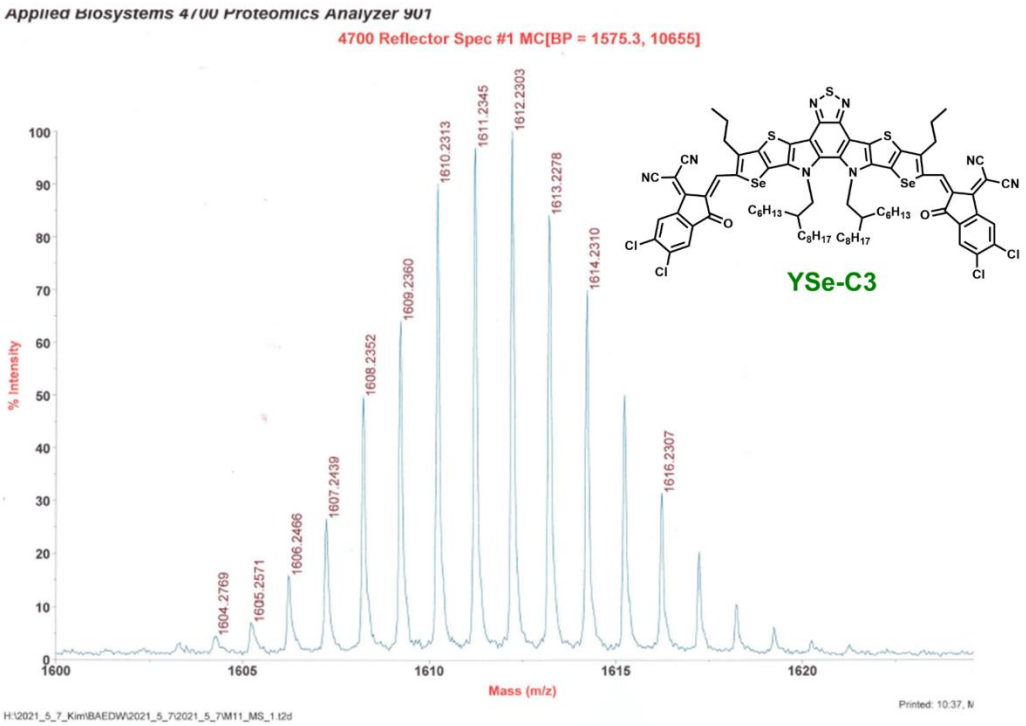
Applied Biosystems 4700 Proteomics Analyzer 901
4700 Reflector Spec #1 MC[BP = 1575.3, 10655]
% Intensity
Mass (m/z)
1604.2769
1605.2571
1606.2466
1607.2439
1608.2352
1609.2360
1610.2313
1611.2345
1612.2303
1613.2278
1614.2310
1616.2307
YSe-C3
H:\2021_5_7_Kim\BAEDW\2021_5_7\2021_5_7\M11_MS_1.fid
Printed: 10:37, M

(b)

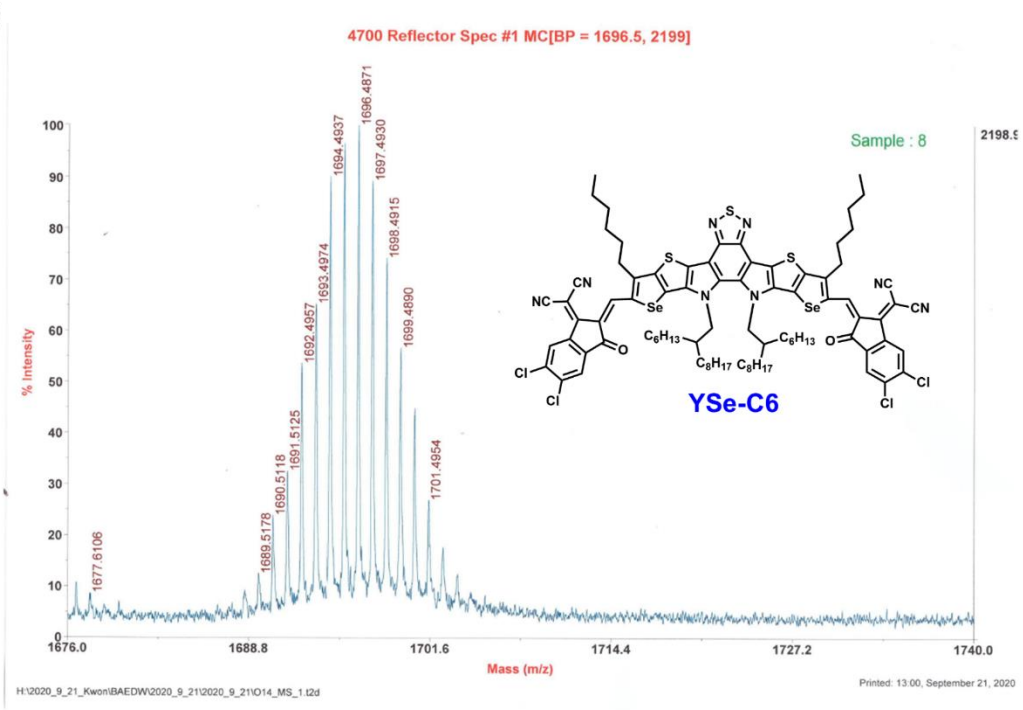
4700 Reflector Spec #1 MC[BP = 1696.5, 2199]
Sample : 8
% Intensity
Mass (m/z)
1677.6106
1689.5178
1690.5118
1691.5125
1692.4957
1693.4974
1694.4937
1696.4871
1697.4930
1698.4915
1699.4890
1701.4954
YSe-C6
H:\2020_9_21_Kwon\BAEDW\2020_9_21\2020_9_21\O14_MS_1.fid
Printed: 13:00, September 21, 2020

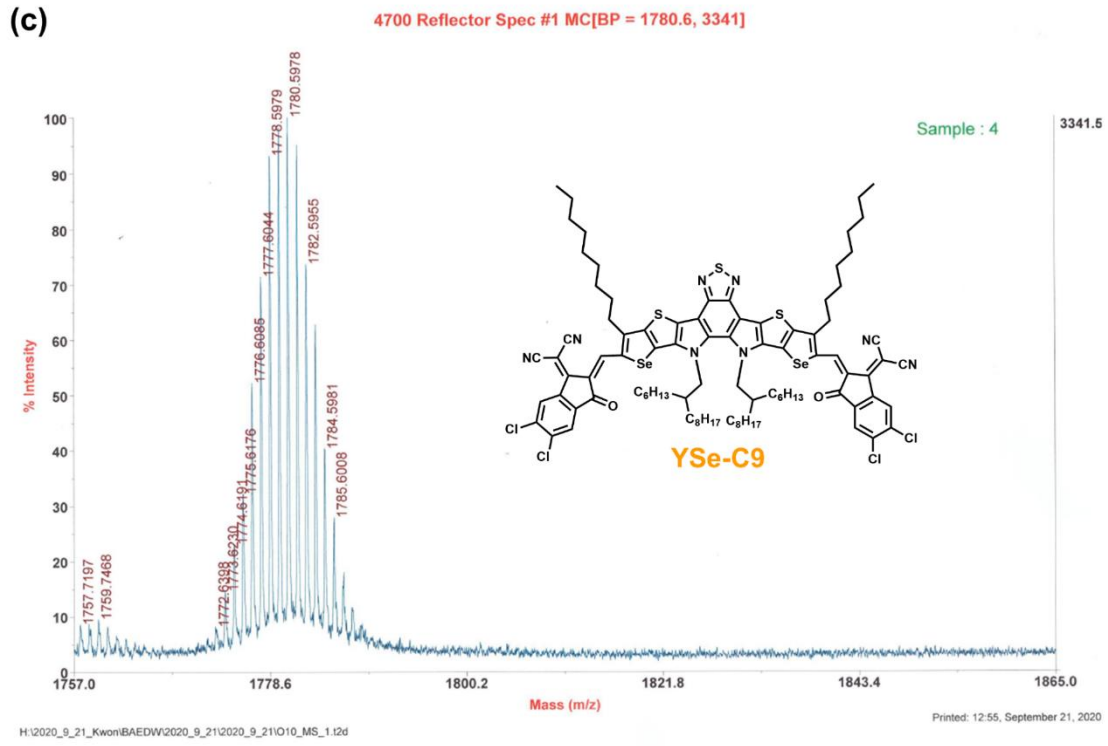

Fig. S3. MALDI-TOF MS analysis of (a) YSe-C3, (b) YSe-C6, and (c) YSe-C9 SMAs.

Table S1. Elemental analysis of YSe-Cx SMAs.

SMAs	C (wt%)		H (wt%)		N (wt%)		S (wt%)	
	Mean	RSD (%)	Mean	RSD (%)	Mean	RSD (%)	Mean	RSD (%)
YSe-C3	61.61	0.07	5.48	0.82	6.84	0.40	6.17	2.97
YSe-C6	62.70	0.73	5.97	0.40	6.49	0.28	5.89	0.50
YSe-C9	63.30	0.05	6.60	0.40	5.89	0.75	5.28	0.02

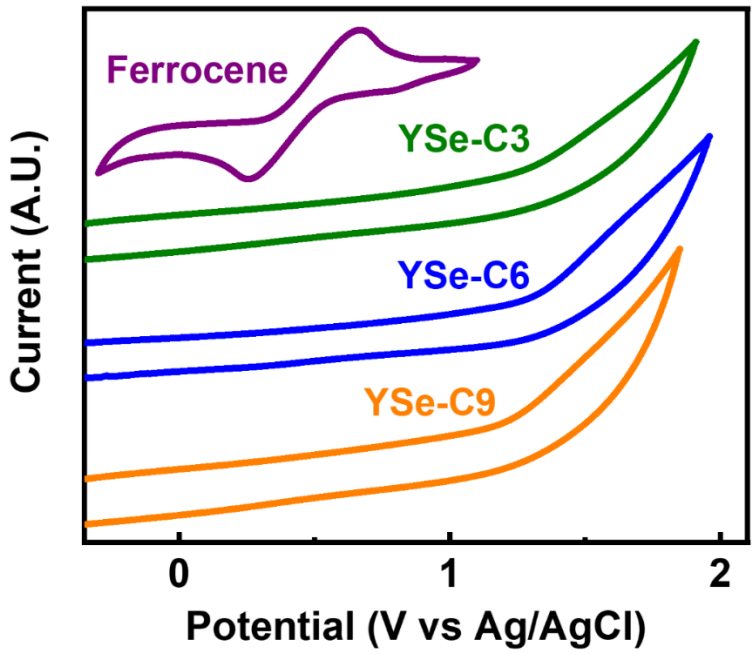

Fig. S4. Oxidation potentials of YSe-Cx SMAs from cyclic voltammetry.

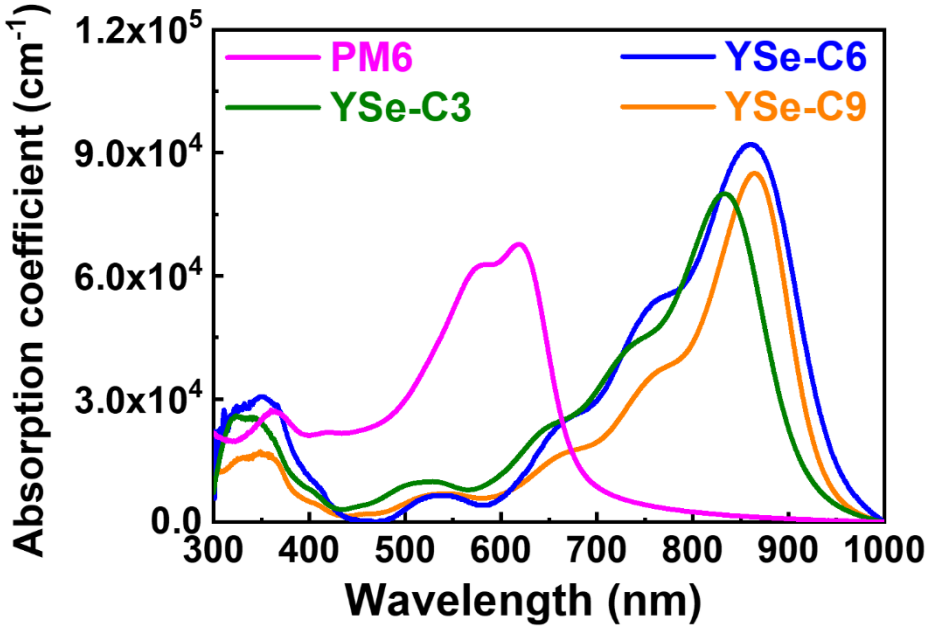

Fig. S5. Absorption coefficients of PM6 and YSe-Cx thin films.

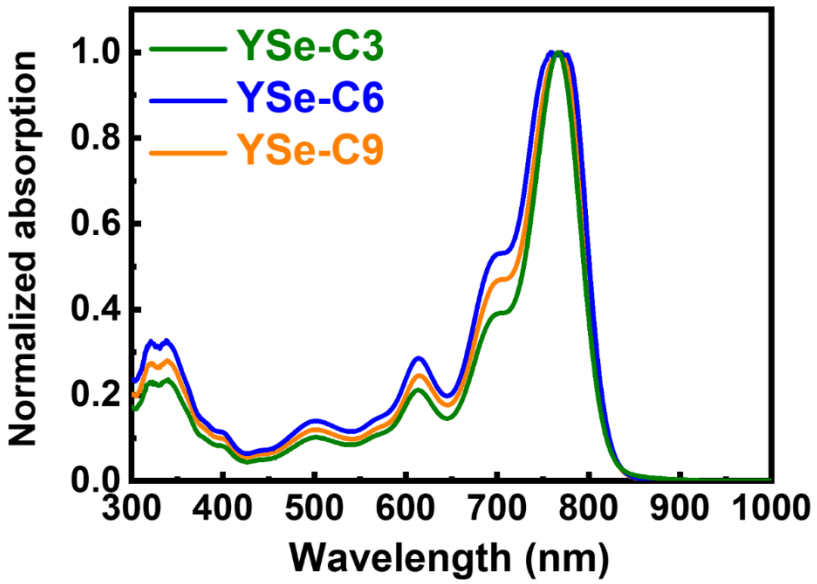

Fig. S6. Normalized UV-Vis absorption spectra of YSe-Cx solution in *o*-xylene.

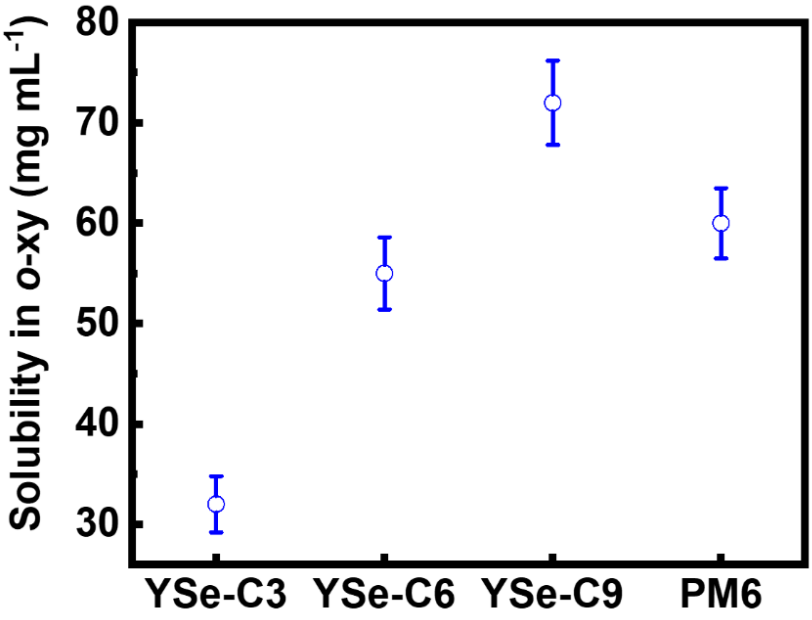

Fig. S7. Solubilities of YSe-Cx SMAs and PM6 in *o*-xylene solvent.

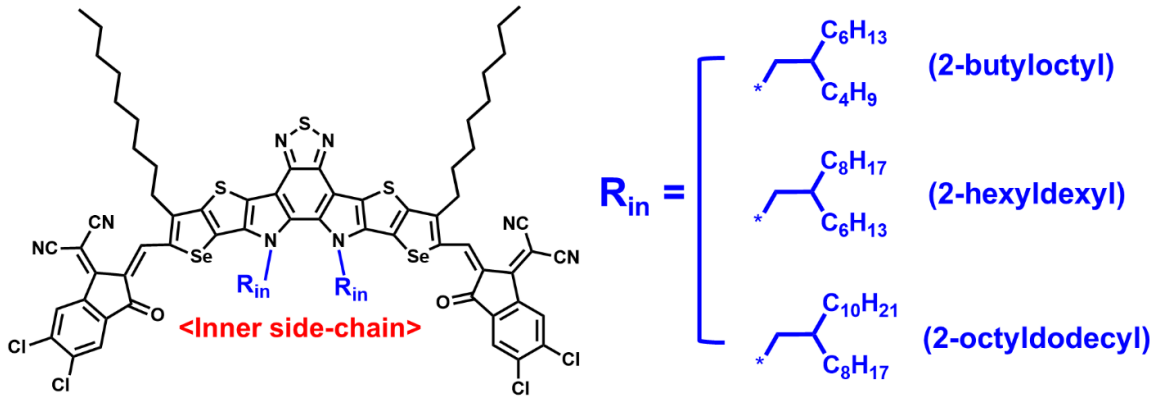

Fig. S8. Chemical structures of YSe-C9 SMAs with different inner side-chains.

Table S2. Photovoltaic properties of optimized PM6:YSe-C9 devices with different inner side-chains.

SMA	Inner side-chain	V_{oc} (V)	J_{sc} (mA cm^{-2})	FF	PCE$_{max}$ (PCE$_{avg}$) (%)
YSe-C9	2-butyloctyl	0.84	23.25	0.70	13.67 (13.19)
	2-hexyldexyl	0.85	23.21	0.72	14.20 (13.77)
	2-octyldodecyl	0.85	23.11	0.69	13.55 (13.01)

Table S3. Photovoltaic properties of optimized PM6:YSe-Cx devices with different non-halogenated solvents.

Processing solvent	SMAs	V_{oc} (V)	J_{sc} (mA cm^{-2})	FF	PCE$_{max}$ (PCE$_{avg}$) (%)
Toluene	YSe-C3	0.84	23.35	0.56	10.97 (10.48)
	YSe-C6	0.84	25.64	0.70	15.08 (14.36)
	YSe-C9	0.85	23.54	0.67	13.32 (12.59)
THF	YSe-C3	0.83	23.57	0.53	10.39 (10.25)
	YSe-C6	0.83	25.43	0.69	14.52 (13.96)
	YSe-C9	0.85	23.66	0.64	12.96 (12.30)

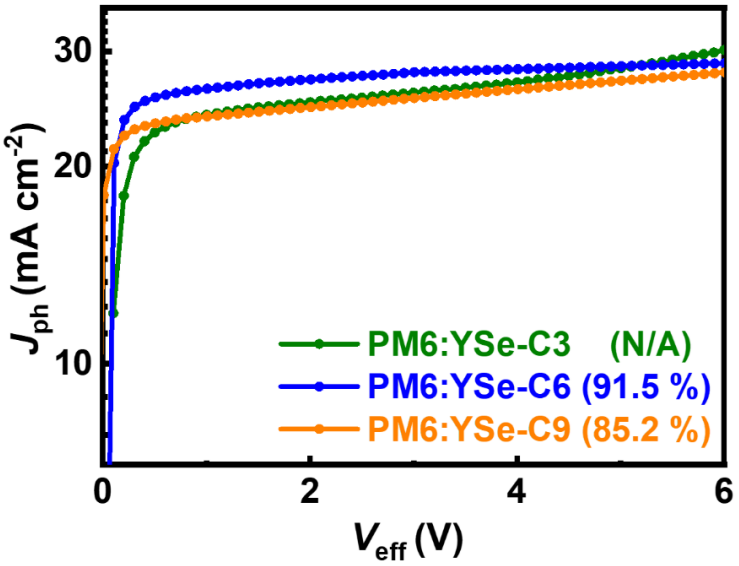

Fig. S9. Photocurrent analysis of PM6:YSe-Cx-based OSC devices.

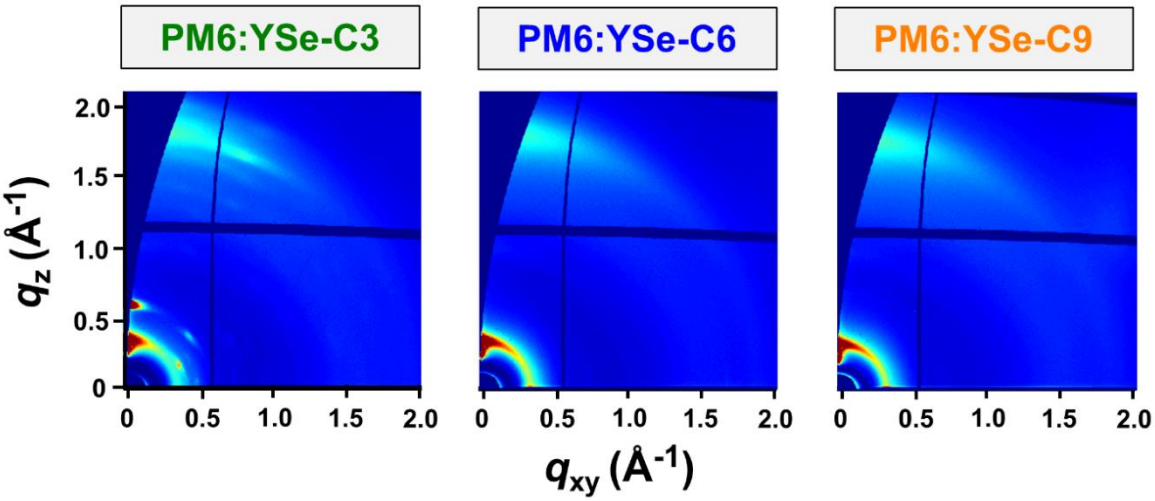

Fig. S10. 2D GIWAXS patterns of PM6:YSe-Cx (x = 3, 6, or 9) blend films.

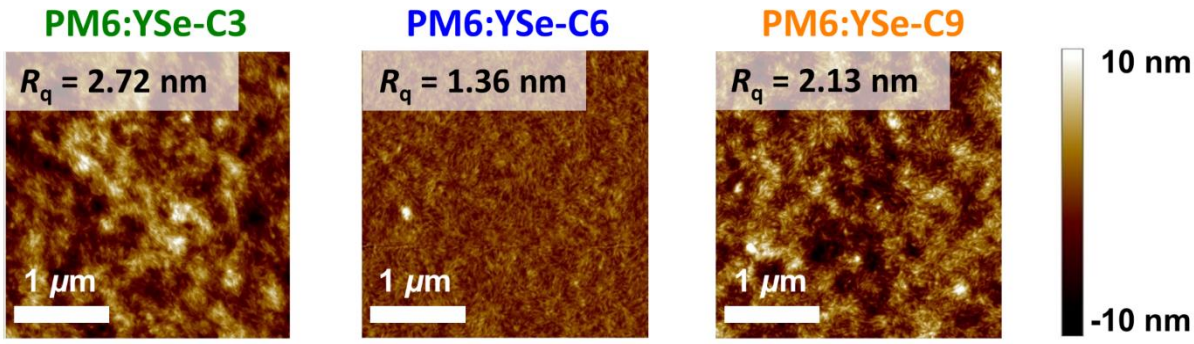

Fig. S11. AFM height images of PM6:YSe-Cx blend films.

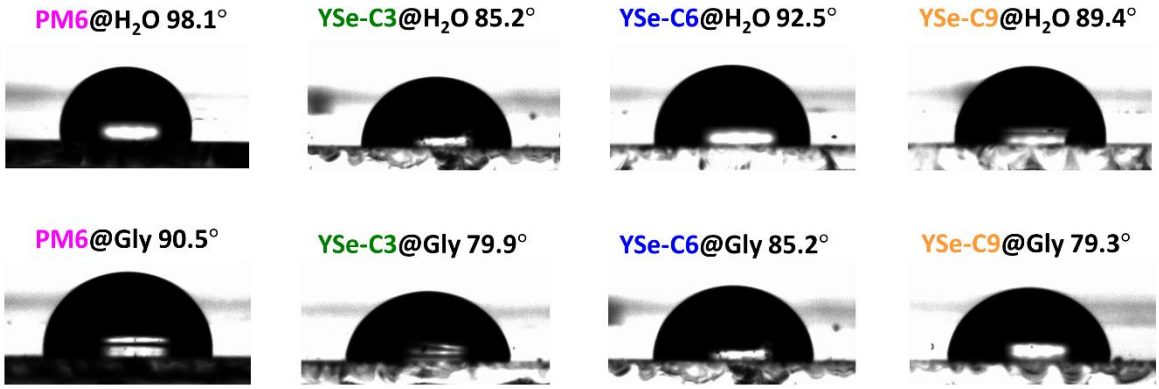

Fig. S12. Contact angle measurements of the neat films of PM6 and YSe-Cx SMAs.

Table S4. Contact angle and surface energy of PM6 and YSe-Cx pristine films processed with *o*-xylene. Flory–Huggins interaction parameters (χ) between PM6 and YSe-Cx in each blend.

Material	θ_{water} (°)	$\theta_{glycerol}$ (°)	Surface Tension, γ (mN m^{-1})	$\chi_{PM6\text{-}SMAs}$
PM6	98.1	90.5	20.96	—
YSe-C3	85.2	79.9	27.42	1.56
YSe-C6	92.5	85.2	23.79	0.25
YSe-C9	89.4	79.3	26.72	0.76

Table S5. Melting temperatures and enthalpies in 1st heating thermogram of YSe-Cx-based pristine and blend films processed with *o*-xylene.

Film materials	T_m (°C)	ΔH_m (J g^{-1})
YSe-C3	282.1	1.83
YSe-C6	275.2	1.51
YSe-C9	259.4	0.94
PM6: YSe-C3	281.7	1.08
PM6: YSe-C6	—	—
PM6: YSe-C9	258.2	0.69

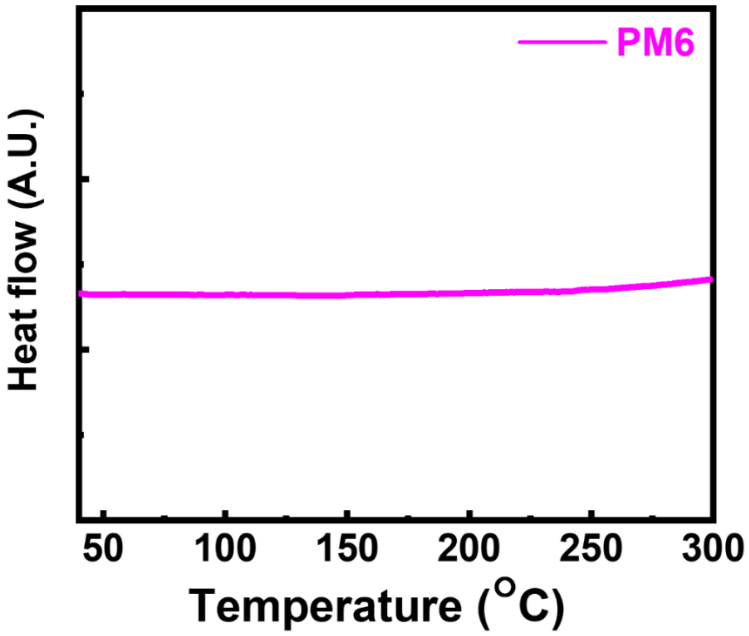

Fig. S13. 1st heating cycle DSC thermogram of PM6 film.

Table S6. Photovoltaic properties of optimized PM6:YSe-Cx devices with different thickness of active layers.

SMA	Active layer thickness (nm)[a]	V_{oc} (V)	J_{sc} (mA cm^{-2})	FF	PCE_{max} (PCE_{avg}) (%)
YSe-C3	114	0.83	23.36	0.60	11.63 (11.14)
	188	0.82	21.46	0.55	9.68 (9.11)
	270	0.81	18.99	0.49	7.54 (7.13)
	370	0.76	16.38	0.42	5.23 (4.77)
YSe-C6	116	0.85	25.94	0.73	16.11 (15.72)
	181	0.83	26.67	0.70	15.54 (14.68)
	285	0.83	26.48	0.68	15.01 (14.31)
	389	0.82	26.63	0.67	14.63 (13.98)
YSe-C9	111	0.85	23.21	0.72	14.20 (13.77)
	194	0.83	24.75	0.62	12.74 (12.06)
	303	0.81	25.10	0.54	10.98 (10.14)
	397	0.80	24.72	0.49	9.69 (9.01)

[a] The average value is obtained from at least 20 different films.

Table S7. SCLC hole and electron mobilities of PM6:YSe-Cx devices with different thicknesses of active layers.

SMA	Active layer thickness (nm)	μ_{h_avg}[a] ($cm^2\ V^{-1}\ s^{-1}$)	μ_{e_avg}[b] ($cm^2\ V^{-1}\ s^{-1}$)	μ_h/μ_e
YSe-C3	114	4.63×10^{-4}	8.81×10^{-5}	5.25
	188	3.11×10^{-4}	5.69×10^{-5}	5.46
	270	2.53×10^{-4}	3.23×10^{-5}	7.83
	370	1.51×10^{-4}	1.63×10^{-5}	9.26
YSe-C6	116	4.58×10^{-4}	3.33×10^{-4}	1.37
	181	2.73×10^{-4}	1.88×10^{-4}	1.45
	285	1.55×10^{-4}	9.87×10^{-5}	1.57
	389	1.04×10^{-4}	6.31×10^{-5}	1.64
YSe-C9	111	3.08×10^{-4}	1.12×10^{-4}	2.75
	194	2.88×10^{-4}	9.71×10^{-5}	2.96
	303	2.58×10^{-4}	9.35×10^{-5}	2.74
	397	2.04×10^{-4}	8.72×10^{-5}	2.61

[a] SCLC hole mobilities were measured from the hole-only devices. [b] SCLC electron mobilities were measured from the electron-only devices.

References

1 J. Yao, B. Qiu, Z.-G. Zhang, L. Xue, R. Wang, C. Zhang, S. Chen, Q. Zhou, C. Sun, C. Yang, M. Xiao, L. Meng and Y. Li, *Nat. Commun.*, 2020, **11**, 2726.

2 D.-M. Smilgies, *J. Appl. Crystallogr.*, 2009, **42**, 1030-1034.

3 J. Rivnay, S. C. B. Mannsfeld, C. E. Miller, A. Salleo and M. F. Toney, *Chem. Rev.*, 2012, **112**, 5488-5519.

4 J. Comyn, *Int. J. Adhes. Adhes.*, 1992, **12**, 145-149.

5 R. Wang, J. Yuan, R. Wang, G. Han, T. Huang, W. Huang, J. Xue, H.-C. Wang, C. Zhang, C. Zhu, P. Cheng, D. Meng, Y. Yi, K.-H. Wei, Y. Zou and Y. Yang, *Adv. Mater.*, 2019, **31**, 1904215.

6 J. A. Emerson, D. T. W. Toolan, J. R. Howse, E. M. Furst and T. H. Epps, *Macromolecules*, 2013, **46**, 6533-6540.

7 S. Nilsson, A. Bernasik, A. Budkowski and E. Moons, *Macromolecules*, 2007, **40**, 8291-8301.

8 J. A. Röhr, D. Moia, S. A. Haque, T. Kirchartz and J. Nelson, *J. Phys. Condens. Matter*, 2018, **30**, 105901.